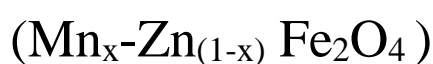
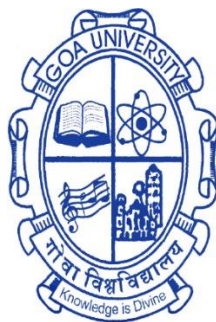


SYNTHESIS, CHARACTERIZATION
AND STUDY OF
SOLID STATE PROPERTIES OF
MANGANESE ZINC FERRITES



An MSc Dissertation report by :

MANASI . A . UGVEKAR



SCHOOL OF CHEMICAL SCIENCES

GOA UNIVERSITY

GOA 403206

April 2022

SYNTHESIS, CHARACTERIZATION AND
STUDY OF SOLID STATE PROPERTIES
OF Mn-Zn FERRITES
($\text{Mn}_x\text{-Zn}_{(1-x)}\text{Fe}_2\text{O}_4$)

A DISSERTATION REPORT

Submitted in Partial Fulfillment
Of
The Degree of MSc (Inorganic Chemistry)

By
Ms. Manasi .A. Ugvekar

To the

School of Chemical Sciences
Goa University
Goa 403206
APRIL 2022

CERTIFICATE

This is to certify that the dissertation entitled “*Synthesis, Characterization and study of solid-state properties of Manganese Zinc Ferrites ($Mn_x-Zn_{(1-x)}Fe_2O_4$)*” is bonafide work carried out by Ms. Manasi Arun Ugvekar under my supervision in partial fulfilment of the requirement for the award of the degree of Master of Science in Chemistry at the School of Chemical Sciences, Goa University.

Prof. Dr. Vidyadatta Verenkar
Guiding Teacher
Dean of School of Chemical Sciences
Goa University

INDEX

Sr. No.	Title	Page No.
1	Introduction	4 -7
2	Literature review of Mn-Zn Ferrites	8 - 18
3	Conclusion	19
4	Acknowledgment	20
5	References	21 - 23

INTRODUCTION

NANOSCIENCE AND NANOTECHNOLOGY

Nanoscience and nanotechnology represent a growing research area, which includes structures, devices, and systems with novel properties and functions due to the arrangement of their atoms on the 1–100 nm scale. The prefix ‘nano’ is referred to a Greek word meaning ‘dwarf’ or something very small and depicts one thousand millionth of a meter (10^{-9} m). Nanoscience is the study of structures and molecules on the scales of nanometers ranging between 1 and 100 nm, and the technology that uses it in practical applications such as devices etc. is called nanotechnology. [1]

FERRITES

A ferrite is a ceramic material that is made up of iron oxide (Fe_2O_3) in larger proportion mixed with metallic elements such as barium (Ba), manganese (Mn), nickel (Ni), zinc (Zn) etc in small proportions. The nature of both the iron oxide and the metal is electrically non-conducting and ferrimagnetic. Ferrimagnetic material is one having unequal opposing magnetic moments which allow such materials to retain spontaneous magnetization[2]. The applications of ferrites are described in the range extending from millimeter-wave integrated circuitry to power handling, simple permanent magnets, and magnetic recording. These applications are well defined on the basis of the properties of ferrites. Apart from these, ferrites also have remarkable applications in the emerging fields of electronic technology and biotechnology.[3]

HISTORY OF FERRITES

The history of ferrite materials began in different centuries before the birth of Christ with the discovery of stones that would attract iron. The large amount of these stones were found in the district of Magnesia in Asia Minor; hence, the minerals were named as magnetite (Fe_3O_4). The first application of magnetite was the “Lodestones” used by early navigators to detect magnetic north. The first scientific study of De Magnete magnetism was published in 1600 by William Gilbert. An electric current in a wire affects a magnetic compass needle was demonstrated by Hans Christian Oersted in 1819. Furthermore, contributions by Faraday, Maxwell, Hertz, and many other scientists in the new field of electromagnetism have developed science greatly. In 1930, Yogoro Kato and Takeshi Takei reported the first ferrite compound at the Tokyo Institute of Technology. Ferrites can be obtained in three different crystal systems by various synthesis methods, and the flexibility to prepare an unlimited number of solid solutions composition to tailor their properties for myriad applications. Ferrites are electrically non-conductive, meaning that they are insulators, and ferrimagnetic means that they can be magnetized and get attracted by a magnet. Lodestone or magnetite is a naturally occurring form of iron oxide i.e. ferrite by

both engineers and geologists. Over 2000 years ago, the Greeks documented the strange properties of lodestone, and almost 1000 years ago, the Chinese research community used it for magnetic compass. Dielectric properties of material demonstrate that even though electromagnetic waves can pass through ferrites, they do not readily conduct electricity. This gives them an advantage over nickel, iron, and other transition metals that already have magnetic properties (“ferromagnetic”) for many applications because these metals also conduct electricity.

CLASSIFICATION OF FERRITES

Ferrites are classified into two categories, based on their magnetic coercivity and the resistance to get demagnetized i.e., soft and hard ferrites. Soft ferrites do not retain their magnetism after being magnetized, such as zinc, cobalt, nickel, manganese, and magnesium ferrites, and hard ferrites are also known as permanent magnets that can sustain their magnetism after being magnetized.

➤ Soft Ferrites

Soft ferrite is a ceramic electromagnetic material that is dark gray or black in appearance with very hard and brittle properties. From the crystallographic aspect, soft ferrites are inverse spinel and belong to the cubic crystal system. In other words, soft ferrites demonstrate a homogenous cubic spinel crystalline structure and are composed of iron oxide with divalent metal oxides. The most important soft ferrites are Mn-Zn ferrites ($\text{MnZnFe}_2\text{O}_4$) and Ni-Zn ferrites ($\text{NiZnFe}_2\text{O}_4$) referring to their applications concern. Magnetic properties of soft ferrites arise from interactions between metallic ions occupying particular positions relative to the oxygen ions in their spinel crystalline structure. When no magnetizing force is present, the magnetic domains are random and the net flux contribution is zero even though local domains are fully magnetized. When a magnetizing force is present, the magnetic domains align in the direction of the magnetizing force, resulting in a large net flux contribution. Soft ferrites are also semiconductors meaning that they are somewhere between conductors and insulators in their ability to conduct electron flow through the material.

➤ Hard Ferrites

In the case of hard ferrites, a strong magnetization retained even after removing the applied magnetizing field, and residual magnetization is stable even if certain strength of the demagnetizing field is applied. These ferrites form a large class of ceramic materials. The colour of hard ferrites varies from dark gray to black and also, they are very hard and brittle. Naturally occurring magnetite is a weak hard ferrite. Hard ferrites possess magnetism, which is essentially permanent. M-type ferrites can be regarded as the more common type of hard ferrites. The most important of these permanent magnetic materials, in practical use, are barium ferrite ($\text{BaO} \cdot 6\text{Fe}_2\text{O}_3$) and strontium ferrite ($\text{SrO} \cdot 6\text{Fe}_2\text{O}_3$). As compared with soft magnetic ferrites, hard magnetic ferrites are weak in structural sensitivity thereby, get influenced by

impurities firing conditions. Two classes of hard magnets, comprising oriented (anisotropic) and nonoriented (isotropic) ferrites, are distinguished.

STRUCTURAL CLASSIFICATION OF FERRITES

❖ Spinel ferrite

Such ferrites are a prototype of naturally occurring ferrites, i.e., $\text{FeO}\cdot\text{Fe}_2\text{O}_3$. The spinel structure is derived from the mineral spinel (MgAl_2O_4 or $\text{MgO}\cdot\text{Al}_2\text{O}_3$), which crystallizes in the cubic system. Analogous to the mineral spinel, the magnetic spinel has the general formula $\text{MeO}\cdot\text{Fe}_2\text{O}_3$ or MeFe_2O_4 where Me is the divalent metal ion. The smallest cell of the spinel lattice that has cubic symmetry contains eight “molecules” of MeFe_2O_4 . The relatively large-sized oxygen ions (radius about 1.4 Å form fcc lattice, and the much smaller metal ions [radii from about 0.7 to 0.8 Å] occupy the spaces between them. In this cubic close-packed structure, two kinds of interstitial sites occur: the tetrahedral and the octahedral sites, which are surrounded by four and six oxygen ions, respectively. In the aforementioned cubic unit cell, 64 tetrahedral (A) sites and 32 octahedral (B) sites are present, of which only 8 and 16, respectively, are occupied by metal ions (called A and B sites). In the mineral spinel, the Mg^{2+} ions are in A sites, and the Al^{3+} ions are in the B sites. $\text{MeO}\cdot\text{Fe}_2\text{O}_3$ has exactly this structure with Me^{2+} in A sites and Fe^{3+} in B sites. Zinc ferrite, the tetrahedral sites are occupied by zinc ions, and nonmagnetic (no unpaired electronic spins), produces no antiferromagnetic orientation of the ions on the octahedral sites that are occupied by Fe^{3+} ions. The Fe^{3+} (B-B) interactions are so weak as to be unimportant; therefore, zinc ferrite is not ferrimagnetic. Both zinc and cadmium ferrites endow this structure which are nonmagnetic, i.e., paramagnetic. Barth and Posnjak found many cases in which the trivalent ions preferred the tetrahedral or A sites and filled these first. Many other ferrites, however, demonstrate the inverse spinel structure in which the divalent ions are on B sites, and the trivalent ions are equally divided between A sites and B sites. Many of the commercially important ferrites such as iron, cobalt, and nickel ferrites confirm inverse spinel structure. Finally, it should be noted that these ferrites can be prepared to contain two different kinds of divalent ions, e.g., $(\text{NiZn})\text{O}\cdot\text{Fe}_2\text{O}_3$. This is called a mixed ferrite although actually it is a solid solution of $\text{NiO}\cdot\text{Fe}_2\text{O}_3$ and $\text{ZnO}\cdot\text{Fe}_2\text{O}_3$. Most of the cubic ferrites used commercially are in mixed ferrite state.

❖ Garnet Ferrite

These are the ferrites that accommodate a large trivalent rare earth ions of large magnetic moments. Garnet ferrites reveal the structure of the silicate mineral garnet. Magnetic garnets crystallize in the dodecahedral or 12-sided structure related to the mineral garnet. The general formula is $\text{Me}_3\text{Fe}_5\text{O}_{12}$. All the metal ions are trivalent in contrast to the other two classes. In the important magnetic garnets, Me is usually yttrium (Y) or one of the rare-earth ions. The crystal structure and the unit cell dimensions of the rare-earth iron garnets were first reported

by Bertaut and Forrat and then by Geller and Gilleo. Hexagonal ferrite structure substitution of Y^{3+} , Al^{3+} , and Si^{4+} obtained for the first time the garnet $Y_3Al_5O_{12}$ free from silicon. The garnet structure is particularly stable because all the sites, occupied by cations, contribute high stability of the compound.

❖ Hexagonal Ferrite

This class of magnetic oxides suggests the magnetoplumbite structure, which comes from the mineral of the same name. The hexagonal ferrites are get defined by $MeFe_{12}O_{19}$, where, Me is usually Ba, Sr, or Pb. The symmetry of the magnetoplumbite structure is hexagonal. Thus, it has a major preferred axis called the c-axis and a-minor axis called the a-axis. The preferred direction is used for a good advantage in permanent magnet material. Most of these compounds are ferrimagnetic, but some are antiferromagnetic. The best known compounds in this class are $BaFe_{12}O_{19}$, $SrFe_{12}O_{19}$, and $PbFe_{12}O_{19}$. Further studies in the ternary system BaO-FeO- Fe_2O_3 have led to the discovery of many other compounds having related hexagonal structures. The complex crystal structures of these compounds were established by Braun.

❖ Ortho ferrites

Perovskite structure is the name given to the atomic arrangement of the oxides of formula RMO_3 , e.g., $BaTiO_3$, $PbTiO_3$ etc. This structure is often acquired by a material, which has a complicated molecular arrangement consistent with cubic symmetry. The rare earth iron perovskites are also known as “orthoferrite”. The structure is orthorhombic rather than cubic. The canting or non-parallel alignment of the antiferromagnetic coupled ions leads to weak ferromagnetism in the perovskite structured materials. These compounds present the structure which is formed by the superposition of a canted spin antiferromagnetic sublattice M and sublattice R.[4]

Literature Review Mn-Zn Ferrites

O. Kamana , D. Kubániováb , K. Knížeka , L. Kubíčkováa, M. Klementováa , J. Kohoutb , and Z. Jirák [5] synthesized Mn-Zn Ferrite particles with a size of ~12nm by hydrothermal synthesis. The present study was devoted namely to five samples with approximate composition $Mn_{1-x}Zn_xFe_2O_4$, where $x = 0.21- 0.63$, that were prepared by a surfactant-free hydrothermal procedure at a rather low temperature of 180°C. Transition to superparamagnetic state was easily controlled by Zn content. Nanoparticles of the selected composition $Mn_{0.62}Zn_{0.41}Fe_{1.97}O_4$ were subjected to neutron diffraction study at 2 K to determine the ferrimagnetic order and in combination with Mössbauer spectroscopy to analyze the cation distribution. The non-zero occupancy of Zn^{2+} in octahedral sites evidenced a metastable distribution, and the supplemental DFT study revealed that the distribution of Mn^{2+} is non-equilibrium as well. The experimental evidence presented in the work suggests that the Magnetic behavior of nanoparticles deviates from their bulk equivalents not only due to finite-size and surface effects but maybe also affected by the occurrence of metastable states, such as non-equilibrium cation distribution.

Zhanyuan Xu, Jinglian Fan, Yong Han, Tao Liu, Hongbo Zhang, Keqi Song, and Chenggong Zhang[6] prepared and characterized polycrystalline Mn–Zn ferrites with different iron concentrations by the nano-in-situ composite method. The phase composition, microstructure, mechanical and magnetic properties of powders and bulk materials were examined. The results presented that the crystallinity of powders decreased with the increasing iron concentration from 46 wt.% to 52 wt.%. The single spinel phase was obtained after sintering at 1200°C of all samples. The iron concentration of 50 wt.% gave the best comprehensive performance of Mn–Zn ferrite. This paper explained the findings of the novel nano-in-situ composite method, which will provoke new thinking and investigation in the research of Mn–Zn ferrite.

V.V. Karansky, A.S. Klimov and S.V. Smirnov[7] studied Structural transformations in Mn–Zn ferrite under low-energy electron beam treatment. Low-energy electron beam treatment of ferrites initiated the process of secondary recrystallization in the near-surface layer. This type of treatment results in a decrease in the concentration of oxygen and zinc in the near-surface layer and causes partial deferritization. Thus Recrystallization was accompanied by a change in the chemical composition of the near-surface layer.

Zhirui Niu, Wenli Feng, Hua Huang, Bo Wang, Lan Chen, Yibo Miao, and Shuai Su [8]synthesized a novel Mn–Zn ferrite/biochar composite (MZF-BC) via green two-step bioleaching and hydrothermal method using waste batteries and pine sawdust. Characterization results indicate that the introduced Mn–Zn ferrite particles are successfully embedded and coated on biochar (BC), and synthesized MZF-BC₅₀ with 50% BC content exhibits the best

performance with a specific surface area of $138.5 \text{ m}^2 \text{ g}^{-1}$, the saturation magnetization of 27.5 emu g^{-1} and CEC value of $53.2 \text{ mmol } 100 \text{ g}^{-1}$. The maximum adsorption capacity of MZF-BC₅₀ for Pb^{2+} was 99.5 mg g^{-1} . It exhibited a good selective Pb^{2+} and Cd^{2+} removal performance in lead-acid battery wastewater. The results illustrated that this newly developed material had low cost and rapid remediation of Pb^{2+} as good application potential.

The recycling of Mn–Zn ferrite wastes through a hydrometallurgical route have been investigated by Kangkang Li, Changhong Peng, and Kaiqi Jiang[9]. A novel recycling route using acid leaching, reduction, purification, co-precipitation, and the traditional ceramic process was applied to process the Mn–Zn ferrite wastes and prepare the corresponding high permeability soft magnetic product. Above 95% of Fe, Mn, and Zn in the waste materials could be recycled in the form of Mn–Zn ferrite products through the hydrometallurgical route. The comprehensive properties of Mn–Zn ferrite prepared from wastes by this route had broader frequency characteristics, higher resistivity, lower loss coefficient, and temperature coefficient as compared to the A102 product (Acme Electronics Corporation, Taiwan). Moreover, the cost of this recycling technology had an economical advantage over the traditional ceramic process.

Caiyin You, Xiaodong Fan, Na Tian, and Jun He[10], investigated electromagnetic microwave absorption of the annealed pre-sintered precursor of Mn–Zn ferrite. X-ray photoelectron spectra (XPS) analyses showed that more Mn^{2+} and Zn^{2+} moved to the surface of particles to form non-stoichiometric $(\text{Mn}, \text{Zn})\text{Fe}_2\text{O}_4$ ferrite under annealing with a partial H_2 , improving the electromagnetic impedance matching. With regards to the original precursor, the lowest reflection loss was around -34.8 dB at 6.3 GHz for a 4 mm thick absorber. After vacuum annealing, the lowest reflection loss was around -34.8 dB at 5.9 GHz for a 4 mm thick absorber. The lowest reflection loss of -47.6 dB was obtained at 13.2 GHz with a 1.85 mm thick absorber after annealing under a partial H_2 . This work presents a convenient way to make a good electromagnetic microwave absorption material beginning from the pre-sintered precursor of Mn-Zn ferrites.

Ping Hu, De'an Pan, Shengen Zhang, Jianjun Tian, and Alex A. Volinsky [11] prepared Mn–Zn soft magnetic ferrite nanoparticles with the mean crystallite size of 25 nm using spent alkaline Zn–Mn batteries as raw materials by means of the multi-step processes consisting of acid leaching, chemical treatment of iron shells and citrate-nitrate precursor auto-combustion. Spent alkaline batteries dismantling, washing, magnetic separation, and crushing steps were consecutively carried out to separate batteries into iron battery shells and other dismantled substances (zinc and manganese compounds). $\text{Zn}(\text{NO}_3)_2$ and $\text{Mn}(\text{NO}_3)_2$ reactant solutions were prepared by dissolving the above substances in HNO_3 . Iron shells were converted into ferric nitrate $\text{Fe}(\text{NO}_3)_3$ by additional chemical treatment. Mn–Zn ferrites were synthesized using the citrate-nitrate precursor auto-combustion method. Obtained Mn–Zn ferrite nanoparticles ($\text{Mn}_{0.5}\text{Zn}_{0.5}\text{Fe}_2\text{O}_4$) had a pure ferrite phase, larger saturation magnetization ($M_s = 60.62 \text{ emu g}^{-1}$), and lower coercivity ($H_c = 30 \text{ Oe}$) compared with the same composition ferrites prepared

by other techniques due to better crystallinity. This Auto-combustion Mn–Zn ferrite synthesis method is a good option for Zn–Mn alkaline batteries recycling.

Kelly Pemartin, Conxita Solans, J. Alvarez-Quintana, and Margarita Sanchez-Dominguez [12] prepared Mn–Zn ferrite nanoparticles with a Spinel structure and a narrow size distribution using the oil-in-water (O/W) microemulsion reaction method under mild conditions. The particle size, crystallinity, and magnetic characteristics of the materials could be tailored by varying the composition of the oil-in-water microemulsion and the nature and concentration of the precipitating agent. Increasing the oil concentration up to 20 wt% (at a constant S: W weight ratio of 25:75), resulted in larger Mn–Zn ferrite nanoparticles (9.4 nm) as compared to those prepared using the microemulsion containing 12 wt% oil; this may be attributed to the higher concentration of precursor in the microemulsion as well as the higher processing temperature. In addition, at constant microemulsion composition (S: W weight ratio of 25:75 and 12 wt% oil phase), larger nanoparticles were obtained when Tetramethylammonium hydroxide (TMAH) was used as a precipitating agent than when using NaOH (5.2 nm vs. 2.4 nm, respectively), which may be due to the higher basic strength and peptizing effect of TMAH on the surface of nanoparticles as well as the concentration of NaOH. XRD studies showed that the obtained materials had the characteristic reflections for Spinel nanocrystalline structure, and the crystallite sizes measured were in good agreement with the results from TEM. The possibility to obtain small NPs with high crystallinity resulted in superparamagnetic behavior of the materials, as well as tunable m_{sn} (saturation magnetization) and T_b (blocking temperature). Their work demonstrates that nanoparticles of complex ceramics such as mixed oxides with a Spinel structure can be obtained by the O/W microemulsion reaction method under mild conditions, without the need for calcination.

In this work Murillo L. Martins, Ariovaldo O. Florentino, Alberto A. Cavalheiro, Rafael I.V. Silva, Dayse I. Dos Santos, and Margarida J. Saeki [13] reported a structural study on the mechanisms of phases formed during the synthesis of Mn–Zn ferrite by the polymeric precursor method. Materials with the composition $Mn_{(1-x)}Zn_xFe_2O_4$, where $0.15 \leq x \leq 0.30$, were synthesized and spinel ferrite was obtained as a single crystalline phase which was formed after a thermal treatment on the precursor resins at 400°C for 2 h in air. After thermal treatments of the precursor powders at 700°C and 1100 °C in air, the samples present great amounts of the undesirable secondary phase hematite (Fe_2O_3), which also shows strong relation with the Zn concentration. On the other hand, thermal treatments on the precursor powders at 700°C for 2h under an N_2 atmosphere lead to powders with only the spinel structure phase. In this case, $x = 0.25$ is the optimum Zn content and highly crystalline and homogeneous samples are obtained. Finally, thermal treatments at higher temperatures jeopardize the stability of the spinel phases even under an N_2 atmosphere.

The nitrate-citrate auto-combustion method was employed by Ping Hu, Hai-bo Yang , De-an Pan , Hua Wang , Jian-jun Tian, Shen-gen Zhang , Xin-feng Wang and Alex A. Volinsky[14]

,to prepare nanocrystalline $Mn_{0.5}Zn_{0.5}Fe_2O_4$ ferrite. The crystalline size of auto-combusted ferrite powders was about 23.6 nm. The effects of heat treatment on the structural and magnetic properties of the prepared ferrite samples were studied. Ferrites decomposed to Fe_2O_3 and Mn_2O_3 after annealing at 550°C in air, which had poor magnetic properties. With continuously increased annealing temperature, Fe_2O_3 and Mn_2O_3 impurities were dissolved when the annealing temperature rose above 1100°C. The sample annealed at 1200°C displayed pure Mn–Zn ferrite phase, which had uniform particle sizes, fine crystallinity, showed larger saturation magnetization ($M_s=48.15 \text{ emu g}^{-1}$), and a lower coercivity ($H_c=51 \text{ Oe}$) than the auto-combusted ferrite powder ($M_s=44.32 \text{ emu g}^{-1}$, $H_c=70 \text{ Oe}$). The sample annealed in argon at 600°C had the lowest coercivity ($H_c=32 \text{ Oe}$) and the largest saturation magnetization ($M_s=56.37 \text{ emu g}^{-1}$). This could be attributed to an increase in phase formation, crystallinity, microstructure, and crystalline sizes.

Yimin Xuan, Qiang Li, and Gang Yang[15] synthesised Mn–Zn ferrite nanoparticles using the hydrothermal precipitation method ($Mn_{1-x}Zn_xFe_2O_4$) from metal sulphate solutions and aqueous ammonia. The pH value of the mixed solution of reagents, the reaction temperature, and reaction time were important factors affecting the quality and size distribution of synthesized particles. The magnetic features of Mn–Zn ferrite nanoparticles ($Mn_{1-x}Zn_xFe_2O_4$) were dependent upon the composition content of Zn. An increase in the substitution degree of Zn could reduce the Curie temperature of Mn–Zn ferrite nanoparticles. The particle magnetization increased with the increase in the composition content of Zn for smaller x, but it decreased with the further increase of the composition content of Zn if $x > 0.6$. The synthesized Mn–Zn ferrite nanoparticles have been used to prepare ferrite ferrofluids. From the estimated saturation magnetization of the ferrite ferrofluid and the nanoparticle diameters, the magnetic moment of Mn–Zn ferrite nanoparticles have been calculated based on the assumption of a single magnetic domain.

Co-precipitation synthesizing technique was adopted by M. Deepty, Ch. Srinivasa, E. Ranjit Kumar, N. Krishna Mohand, C. L. Prajapat, T. V. Chandrasekhara Rao, Sher Singh Meena, Amit Kumar Verma, and D. L. Sastry [16] to prepare manganese doped zinc ferrite nanoparticles with varying concentrations of 0.5, 0.6, and 0.7. The consistency of stoichiometry of compositions in the ferrite samples were proved by EDX. XRD patterns confirmed the ferrite phase in the investigating samples. The experimental lattice parameter (8.412–8.438 Å) was increasing and crystallite size (7.6–6.4 nm) appeared to be decreasing with the substitution of Mn^{2+} . The grain size (1.1µm) in the sample ($x=0.7$) with smaller crystallites (6.4 nm) was found to be bigger than that of the remaining compositions ($x = 0.5, 0.6$). A small amount of secondary phase $\alpha\text{-Fe}_2\text{O}_3$ was present in the ferrite sample with composition $x = 0.6$. It may be due to the change in free energy released during the preparation process. The formation of grains due to the agglomeration of crystallites seems to be affecting the experimental lattice parameter. Present ferrite systems formed cubic spinel structure as confirmed from XRD and FTIR. The secondary phase observed in the composition $x=0.6$ were not showing any effect on the ESR parameters, but these seemed to be influenced by the core-shell morphology of

nanoparticles and cation redistribution in the prepared ferrite systems. The study of present ferrite nanoparticles showed that the present ferrite systems can be potential candidates for biomedical applications as well as gas sensing applications.

The electromagnetic and microstructural properties of nanocrystalline spinel ferrite ($\text{Mn}_{1-x}\text{Zn}_x\text{Fe}_2\text{O}_4$) ($x = 0.0 - 1.0$) prepared by the novel route of combustion method were investigated by Ming-Ru Syue, Fu-Jin Wei, Chan-Shin Chou and Chao-Ming Fu [17]. The morphology and microstructure were characterized by scanning electron microscopy and X-Ray diffraction, respectively. The magnetic properties were measured using a vibrating sample magnetometer. The results showed that the permittivity, saturated magnetization and coercivity increased as the content of manganese was raised. The studies of complex impedance spectra by an equivalent circuit model were used to evaluate the AC electrical conduction mechanism. Solvent's weight ratio and the homogeneity of the reagent mixture were critical for the synthesis of ferrite with pure phase and excellent electromagnetic properties. The results showed that synthesized Mn-Zn ferrites with low conductivity and good magnetic properties have excellent potential for applications in electromagnetic devices.

The high-energy gamma irradiation-induced structural transformations in nanocrystalline $\text{Mn}_{1-x}\text{Zn}_x\text{Fe}_2\text{O}_4$ ($x = 0, 0.25, 0.5, 0.75, \text{ and } 1$) samples synthesized by solution combustion method using a mixture of fuels were studied by Jagadeesha Angadi V., Anupama A. V., R. Kumar2, H. K. Choudhary, S. Matteppanavar, H. M. Somashekarappa, Rudraswamy B, and B. Sahoo[18]. All samples were given exposure to 50kGy of gamma radiation. Results confirmed that a dosage of 50 kGy was high enough to break the chemical bonds and produce atomic diffusion in the nanocrystalline materials. The γ -irradiation decomposed the single cubic spinel (Fd-3m) structure of the samples into new stable phases. The pure ZnFe_2O_4 sample retained its phase while the pure MnFe_2O_4 sample transformed to Mn_2O_3 and Fe_{1-x}O phases. Although, SEM images confirm the change in morphology of the pure ZnFe_2O_4 sample after γ -irradiation, the XRD and Mössbauer spectroscopy confirmed the retention of the crystal structure. This demonstrates that the ZnFe_2O_4 phase was structurally quite stable and it does not transform to any other phase even at the radiation dose of 50 kGy (at a rate of 9.5 kGy/h). For the samples with intermediate Zn-content, γ -irradiation facilitates the formation of stable $\alpha\text{-Fe}_2\text{O}_3$ and ZnFe_2O_4 phases, along with the amorphous MnO phase. The scanning electron micrographs demonstrated the complete change of the sample morphology with a fusion of the particles after γ -irradiation. According to the results, the Mn-ferrite and Mn-Zn ferrites were not only magnetically soft, but also the Mn atoms are metastable (compared to Zn atoms) in their sites.

In the present study, M.A. Gabal, R.S. Al-luhaibi, and Y.M. Al Angari [19] used spent Zn-C dry batteries as a source of Zinc, manganese, and iron for preparing manganese-zinc ferrites through the citrate sol-gel auto-combustion method. The contents of the battery were leached with nitric acid and the chemical composition was evaluated using atomic absorption

spectroscopy (AAS). Stoichiometric amounts of the respective metal nitrates were used to tune the proper compositions to reach $Mn_{1-x}Zn_xFe_2O_4$ (with $x = 0.2-0.8$). Thermal analysis measurements (DTA-TG-DSC) were used to characterize the thermal decomposition reaction of the synthesized gel precursor. Single-phase cubic ferrites were shown by the XRD pattern of the prepared ferrites. The changing of the lattice parameters with increasing Zn-content could be explained based on the relative ionic radius of the respective metals and their cation distribution. In addition, X-ray density showed a relative dependence on both molecular weight and volume of the investigated sample. Agglomerated particles with an average crystallite size that agrees well with the XRD pattern were revealed by TEM images. FT-IR spectra showed two absorption bands characteristic of cubic ferrites. Their changing behavior with Zn-content agrees well with that calculated for tetrahedral and octahedral sites ionic radii, which suggests proper cation distribution. Hysteresis loop measurements demonstrated ferromagnetic characters for all the analyzed samples. The changes in the magnetic properties are influenced by cationic stoichiometry. Zn-substitution affected both the structural and magnetic properties of the prepared ferrites.

M.A. Gabal, R.S. Al-luhaibi, and Y.M. Al Angari [20] investigated a novel recycling route using acid leaching, reduction, and gelatin method applied to recycle spent Zn-C batteries into more valuable magnetic nanocrystalline ferrites; $Mn_{1-x}Zn_xFe_2O_4$ (with $x = 0.2 - 0.8$). Nano-crystalline Mn-Zn ferrites with crystallite sizes in the range of 21– 41 nm were prepared. The investigated ferrites were characterized using XRD, TEM, FT-IR, and VSM measurements. The obtained magnetization values were significantly lower than that of the bulk ferrite and showed a gradual increase with increasing Zn-substitution with an obvious decrease at $x = 0.6$. On the other side, an opposite trend was exhibited by coercivity. The effect of Zn-substitution on both structural and magnetic properties opened the way to suggest proper cation distributions.

M.A. Gabal, R.S. Al-luhaibi, and Y.M. Al Angari [21] synthesized single-phase nano-sized $Mn_{1-x}Zn_xFe_2O_4$ ferrites ($x = 0.2-0.8$) with cubic spinel structure from spent Zn-C batteries through the urea auto-combustion route. The obtained lattice parameter, infrared band positions, saturation magnetization, and coercivity were used to determine the proper cation distribution of the system. Both the structural and magnetic properties were found to be affected by the Zn-substitution. The magnetic measurements revealed that the change in the values of saturation magnetization with increasing Zn-content can be explained according to the cation distribution while, that in the coercivity values can be defined based on the magneto-crystalline anisotropy. All the analyzed ferrites samples (except for that with $x = 0.6$) showed reasonably good magnetic properties suggesting the feasibility to synthesize Mn-Zn ferrites with improved properties from spent Zn-C batteries.

The density, microstructure, and magnetic properties of non-doped Mn-Zn ferrite nanoparticles sintered compacts were analyzed by WANG Xin, CUI Yinfang , WANG Yongming, HAO

Shunli, and LJU Chunjing[22]. The compacts of non-doped Mn-Zn ferrite nanoparticles were sintered by the segmented-sintering process at a lower sintering temperature. The density of sintered samples were measured by the Archimedes method, and the phase composition and microstructure were examined by XRD and SEM. The ferrite magnetic measurements of the sintered Mn-Zn were carried out with Vibrating Sample. Their study concluded that the density of sintered compacts increased with the rise in sintering temperature, achieving 4.8245 g.cm^{-3} when sintered at 900°C , which is the optimal density of Mn-Zn functional ferrite and from the fractured surface of sintered samples, it was seen that the grain grows well with smaller grain size and homogeneous distribution. Moreover the samples sintered at 850°C had better magnetic properties.

Nanocrystalline Mn–Zn ferrite spinel powders were synthesized by I. Szczygieł , K. Winiarska , A. Bien´ko, K. Suracka , and D. Gaworska-Koniarek [23] by combined coprecipitation and sol-gel autocombustion methods. The effect of the precursors used in the sol-gel autocombustion synthesis on the ferrite’s structural and magnetic properties were studied. XRD, FTIR, TEM, and SQUID magnetometer measurements were used to characterize the synthesized ferrite powders. All ferrite powders formed from different precursors, after sol-gel autocombustion, were pure spinel phase, without any secondary phases. Studies have shown that the choice of a precursor for the sol-gel autocombustion method greatly influences both the synthesis process conditions and the properties of the synthesized materials, such as microstructure, surface quality, and magnetic properties. Sodium hydroxide, when used as the precipitating agent gave a high precipitation yield of the main ferrite components. But as compared to the precursor of the combustion process, more nitric acid and citric acid was required for the sol-gel autocombustion synthesis, by means of which the combustion process was more rapid. The obtained ferrite nanopowders had larger particles, which formed quite loose agglomerates non-uniform in shape. The (2 M sodium hydroxide solution) P1/OH powder was easily compressible and the sintered material was characterized by a relatively constant magnetic permeability in a quite wide frequency range. Ammonium oxalate as the precipitating agent favored the formation of a fine-crystalline precipitate which was easily filterable, but the precipitation yield was lower than that for the sodium hydroxide. As the precursor in combustion synthesis, oxalate precipitate allowed adopting milder combustion synthesis conditions. This favored the formation of fine-grained particles, but smaller amount of gases released during combustion caused the formation of hard agglomerates. The nano-sized Mn–Zn ferrites obtained as a result of combustion were ferrimagnetic and were characterized by high Curie temperature and magnetization. The P1/OH sample was characterized by a greater value of M_s (112 emu/g), whereas the (2M ammonium oxalate) P2/C2O4 had higher T_c ($719 \pm 5 \text{ K}$). The high (for ferrites) coercivity (~ 80 and $\sim 65 \text{ Oe}$ for the P1/OH and the P2/C2O4, respectively) may be due to the considerable magnetocrystalline anisotropy, which often results in higher power losses as a function of frequency. The shape of the FC/ZFC curves specified a wide grain size distribution and the high value of T_B was due to the considerable percentage of larger grains or their agglomerates. The proposed method can be successfully used to synthesize nano-sized Mn–Zn ferrites. Because of defects in the

structure (porosity, hard agglomerates), the obtained ferrites had a slightly inferior magnetic property than industrial materials and the sintering conditions must be improved in the future, but they are also excellent catalysts.

Structural and Magnetic properties of Mn–Zn ferrite thin films with various Zn content fabricated by alternately sputtering were investigated by Yan Liu, Jiangwei Cao, and Zheng Yang [24]. $Mn_{1-x}Zn_xFe_2O_4$ thin films with various Zn content were deposited on Si (1 0 0) substrate by alternately sputtering from two targets with the composition of $MnFe_2O_4$ and $ZnFe_2O_4$, respectively. The as-deposited films obtained were amorphous. After being annealed in the vacuum furnace with air pressure $P_{Air} = 2 \times 10^{-1}$ Pa at a suitable temperature, crystalline Mn–Zn ferrite films were obtained. The Mn–Zn ferrite films annealed at 550–600°C showed the best magnetic properties. For Mn–Zn ferrite films of different compositions, the saturation magnetization M_s increased firstly and then decreased, but coercivity H_c decreased monotonously with increasing Zn content. At $x = 0.40$, M_s of $Mn_{1-x}Zn_xFe_2O_4$ films showed a maximum 420 kA/m. The soft magnetic properties of the Mn–Zn ferrite thin films were improved by the use of $ZnFe_2O_4$ underlayer, which can reduce the strain in the films and hamper the diffusion between the Si substrate and Mn–Zn ferrite thin film.

In the study conducted by T-H. Kim, G. Senanayake, J-G. Kang, J-S. Sohn, K-I. Rhee, S-W. Lee, and S-M. Shin [25], reductive sulfuric acid leaching with H_2O_2 , and oxidative alkaline coprecipitation with O_2 were applied to recover a valuable zinc manganese ferrite product from spent zinc-carbon batteries. Leaching with 2 mol dm^{-3} H_2SO_4 and 0.39 mol H_2O_2 at a solid/liquid ratio of 1:10, 60 °C, and 200 rpm extracted 97.9% Mn, 98.0% Zn, and 55.2% Fe. The leach liquor composition was then adjusted to an Mn:Zn: Fe molar ratio of 1:1:4 suitable for producing $MnZnFe_4O_8$ ferrite powder by adding Mn(II), Zn(II), and Fe(II) sulfates. Mn–Zn ferrite nanoparticles were successfully synthesized from the leach liquor at 80 °C by sparging with 1.3 $dm^3 min^{-1}$ O_2 gas over 60 min. The synthesized Mn–Zn ferrite powder had a particle size of 20 nm with a spinel structure. A vibrating sample magnetometer (VSM) was used to evaluate the magnetization of Mn–Zn ferrite. Saturation magnetization ranged from 39 to 91 emu/g depending on zinc content ($x = 0.2–0.8$).

Abnormal morphology of nanocrystalline Mn–Zn ferrite sintered by pulse electric current sintering was studied by Jianhua Zhang, Liming Yu, Shujuan Yuan, Shouhua Zhang, and Xinluo Zhao [26]. Nanocrystalline manganese–zinc (Mn–Zn) ferrite powders prepared by the sol-gel auto-combustion method were sintered to form bulk ferrite by pulse electric current sintering technique (PECS). The sample phase, before sintering and after sintering, was carried out by X-ray diffraction (XRD). Scanning electron microscopy (SEM) was used to observe the morphology of the sample. The sample had a spinel structure both before and after PECS. When sintering with the special ring-shaped graphite die, a special morphology was observed. Although most of the samples after PECS had normal grains, near the top surface, there was a

coating without grain boundary; near the medial surface, the grains were slightly oblique and strip-shaped in the radial direction. It may be the cooperation of pressure, temperature, and electromagnetic field that form the abnormal morphology.

The electromagnetic absorbing behaviors of a thin coating fabricated by mixing Mn–Zn ferrite with epoxy resin (EP) were studied by Wenjie Wang, Chongguang Zang, and Qingjie Jiao [27]. $Mn_{1-x}Zn_xFe_2O_4$ ($x = 0.2, 0.5, \text{ and } 0.8$) was designed and synthesized with citrate acid as a complex agent by the sol-gel combustion method. SEM and XRD revealed the fine morphology and pure crystalline structure of the samples. The applicability of the fabricated composite coating for electromagnetic microwave absorption was evaluated in terms of its complex permeability, complex permittivity, and reflection loss. The experimental results showed that a satisfactory value of -17 dB at 800 MHz and the minimum absorption of 10 dB above 700 MHz could be obtained by the $Mn_{0.8}Zn_{0.2}Fe_2O_4/EP$ composite coatings. It was proposed that the prepared composites could potentially be applied in an electromagnetic microwave absorbing field due to the higher reflection loss and broadened absorbing band in the low frequency (10 MHz to 1 GHz).

The aim of this study was to evaluate the influence of the urea and glycine fuels on the synthesis of Mn–Zn ferrite by combustion reaction which was investigated by A.C.F.M. Costa, V.J. Silva, C.C. Xin, D.A. Vieira, D.R. Cornejo, and R.H.G.A. Kiminami [28]. Characterization of powders were carried out by X-ray diffraction (XRD), nitrogen adsorption (BET), scanning and transmission electron microscopy (SEM and TEM), and magnetic measurement of $M \times H$ curves. The X-ray diffraction patterns showed that the samples containing urea resulted in the formation of crystalline powders and the presence of hematite as a secondary phase. The samples containing glycine presented only the formation of crystalline and monophasic (Mn, Zn) Fe_2O_4 . The saturation magnetization was 3.6 and 75 emu/g and the average crystallite size was 18 and 35 nm, respectively, for the samples containing urea and glycine. The samples synthesized with glycine fuel showed better magnetic properties for application as soft magnetic devices.

The effects of annealing temperature and manganese substitution on the formation, microstructure, and magnetic properties of $Mn_{1-x}Zn_xFe_2O_4$ (with x varying from 0.3 to 0.9) through a solid-state method have been investigated by M.M. Hessien, M.M. Rashad, K. El-Barawy and I.A. Ibrahim [29]. The correlation of the microstructure and the grain size with the magnetic properties of Mn–Zn ferrite powders were also reported. X-ray diffraction (XRD), a scanning electron microscope (SEM), and a vibrating sample magnetometer (VSM) were utilized to study the effect of variation of manganese substitution and its impact on crystal structure, crystalline size, microstructure, and magnetic properties of the ferrite powders formed. The XRD analysis showed that pure single phases of Mn–Zn ferrites were obtained by increasing the annealing temperature to 1200–1300°C. Increasing the annealing temperature to

$\geq 1300^\circ\text{C}$ led to abnormal grain growth with inter-granular pores and this led to a decrease in the saturation magnetization. Moreover, an increase in the Mn^{2+} ion substitution up to $x = 0.8$ increased the lattice parameter of the formed powders due to the high ionic radii of the Mn^{2+} ion. Mn–Zn ferrite phases were obtained and the peak positions were shifted by substituting manganese. The average crystalline size was decreased by increasing the substitution by manganese up to 0.8 and increased by increasing the annealing temperature. The average crystalline size was in the range of 5 – 137.3 nm. At an annealing temperatures of 1200–1300 $^\circ\text{C}$, the saturation magnetization of the Mn–Zn-substituted ferrite powders increased continuously with an increase in the Mn concentration up to 0.8. Further increment of Mn substitution up to 0.9 led to a decrease in saturation magnetization. The saturation magnetization increased from 17.3 emu/g for the $\text{Mn}_{0.3}\text{Zn}_{0.7}\text{Fe}_2\text{O}_4$ phase particles produced to 59.08 emu/g for $\text{Mn}_{0.8}\text{Mn}_{0.2}\text{Fe}_2\text{O}_4$ particles.

Synthesis of wide-application Zn–Mn ferrite soft magnetic materials using spent Zn–Mn batteries as starting raw materials was investigated by Yinan Song, Qifei Huang, Zhirui Niu, Jie Ma, Baoping Xin, Shi Chen, Jiulan Dai, and Renqing Wang [30]. The series processes of reductive acid leaching and oxidative co-precipitation and high-temperature calcination or hydrothermal reaction were usually employed to carry out the conversion. In this work, a novel multi-step process of bioleaching and coprecipitation at 30 $^\circ\text{C}$ and boiling reflux at 100 $^\circ\text{C}$, which was characteristic of low cost, environmental friendliness, and energy-saving, was attempted to achieve the conversion for the first time. The results showed that the synthesis of Zn–Mn ferrite using bioleaching liquor as a precursor was feasible. NaOH was the best co-precipitator for manufacturing the soft magnetic material from bioleaching liquor compared with NaHCO_3 and NH_4HCO_3 . Higher pH value of the second co-precipitation at 13.0, higher total concentration of $\text{Mn}^{2+} + \text{Zn}^{2+} + \text{Fe}^{2+}$ at 2.0 mol/l and longer reflux time at 5 h were essential for greater magnetization and better crystallinity. Under optimum conditions, this novel multi-step process harvested soft magnetic material with the highest saturation magnetization of 102 $\text{emu} \cdot \text{g}^{-1}$, offering an alternative to convert spent Zn–Mn batteries into Zn–Mn ferrite.

A. Angermann, E. Hartmann, and J. Töpfer [31] synthesized a mixed Mn–Zn–Fe carbonate by precipitation of metal ions with ammonium carbonate and control of $\text{pH}=7$. Thermal decomposition of the carbonate precursor at 500 $^\circ\text{C}$ in air resulted in the formation of nanocrystalline Mn–Zn ferrite powders. The carbonate was identified by XRD and IR spectroscopy. Ferrite particles had mean crystallite size of 14 nm with a specific surface of 74 m^2/g . The morphology of the spinel ferrite particles resembled that of the carbonate crystals, and the ferrite particles were loosely agglomerated. The magnetization at 5K of the Mn–Zn ferrite powders (66 emu/g) was smaller than the saturation magnetization of the bulk material. Hysteresis loop measurements indicated ferrimagnetic behavior at 5 and 298 K with a small coercivity at room temperature.

Syoichi Sakurai, Satoshi Sasaki, Maki Okube, Hiroki Ohara, and Takeshi Toyoda [32] investigated cation distribution and valence state in manganese zinc ferrite with the synchrotron X-rays, where the two-wavelength anomalous dispersion (TWAD) technique of X-ray diffraction was used for Fe K and Zn K absorption edges, at wavelengths of 1.7535 and 1.2934 Å respectively. The results displayed that a single crystal of $Mn_{0.80}Zn_{0.18}Fe_{2.02}O_4$ grown at $T = 1373$ K had an inverse-spinel ingredient, where 11% of Mn and 44% of Zn ions occupied the octahedral B sites of spinel ferrite. Manganese zinc ferrite synthesized at $T = 1873$ K had quite a different cation distribution and a typical normal-spinel structure. The chemical shifts in Mn K, Zn K and Fe K X-ray absorption near-edge structure (XANES) spectra support that only Mn^{2+} , Zn^{2+} and Fe^{3+} ions exist in the manganese zinc ferrite. From a combination study of XANES and X-ray magnetic circular dichroism (XMCD) spectroscopy at the Mn K edge, it suggest that Mn^{2+} ions occupied both tetrahedral A and octahedral B sites. The chemical formula determined in this study was described as $(Mn_{0.71}^{2+}Zn_{0.10}^{2+}Fe_{0.19}^{3+})[Mn_{0.09}^{2+}Zn_{0.08}^{2+}Fe_{1.83}^{3+}]O_4$.

Lu Xiao, Tao Zhou, and Jia Meng [33] used spent alkaline Zn–Mn batteries as raw materials to prepare 12-nm nanocrystalline Mn–Zn ferrite ($Mn_{0.6}Zn_{0.4}Fe_2O_4$) particles via a multi-step process consisting of acid leaching, co-precipitation and hydrothermal processing. A relationship between Fe(II), Mn(II), Zn(II) concentration and the pH value was obtained through thermodynamic analysis of the Fe(II)–Mn(II)–Zn(II)–NaOH–H₂O system, it showed that all ions could be precipitated completely at pH value of 10–11. Experiments showed that longer reaction time and higher processing temperature might contribute to better crystallization of the ferrite particles. The recommended optimal conditions were: 200°C and 9h.

Ade Yusmar, Linda Armitasari and Edi Suharyadi [34] studied dielectric properties of $Mn_{1-x}Zn_xFe_2O_4$ spinel ferrite with different Zn concentration ($x = 0.2, 0.3, 0.4, 0.5, 0.6, 0.7, 0.8$) over a wide frequency range 5–120 kHz by impedance spectroscopy. The formation of mixed spinel phase structure was revealed by X-ray diffraction (XRD). The crystallite sizes were in the range of 15 to 30 nm. The lattice parameter of $Mn_{1-x}Zn_xFe_2O_4$ spinel ferrite at $x = 0.3$ was 8.559 Å and then decreased by increasing Zn concentration. This was due to the replacement of larger radius ion of Mn^{+2} . The particles size decreased by increasing Zn concentration. The dielectric parameter such as real dielectric constant, imaginary dielectric constant, loss tangent and AC conductivity decreased by increasing Zn concentrations. Zn concentration would affect availability of ferrous and ferric ions in the octahedral sites which was preferentially occupied by Zn^{2+} ion. The dielectric constant exhibited decreasing trend with increasing frequency while loss tangent and AC conductivity increased by increasing frequency.

CONCLUSION

This report has briefed the types, synthesis methods, and solid-state properties of Manganese Zinc ferrite materials. The synthesis of Mn-Zn ferrite particles has increased in last ten years and most progress can be seen in the year 2016. Due to the fascinating properties of Mn-Zn ferrites among the class of soft ferrites like high value of saturation magnetization, low value of coercivity, high initial permeability, narrow size distribution of the ferrite particles, low remenant magnetization, the researchers are taking interest in the synthesis of these ferrites. The co-precipitation and sol-gel method were best for getting the fine crystallite size among all synthesis techniques. The XRD pattern of the Mn-Zn ferrites had characteristic peaks showing the cubic spinel phase having $Fd3m$ phase group. FTIR spectra confirmed the spinel phase of the ferrite nanoparticles having tetrahedral and octahedral sites. Also, for obtaining the low value of coercivity sol-gel method was preferred. Generally, Mn-Zn ferrites have a lot of applications including biomedical field, electronic devices, for making radar absorbing materials, for making ferrofluids etc. In the context of use of nanoparticles in the pandemic outbreak, such as in the recent COVID-19, Mn-Zn soft ferrites can play a significant role in the development of high contrast imaging dyes for viral strains in body fluids. Perhaps Mn-Zn can also serve as a candidate nanomaterial for developing nanomaterial based medicines and therapeutics. If researchers and engineers who are concerned with ferrites take a deeper look at the future aspects of ferrites and devote themselves to the subjects of great value, the future of ferrites will experience a steady and more advanced prosperity in science and technology, and their industries will be continue to grow in the future.

ACKNOWLEDGEMENT

It was indeed a great sense of joy achieved to see this project completed. It has been a very faithful and enjoyable learning experience for me. The project on which I have worked, entitled “*Synthesis, Characterization, and study of solid-state properties of Manganese Zinc Ferrites ($Mn_x-Zn_{(1-x)}Fe_2O_4$)*” could have not been possible without significant guidance and a lot of hard work. The fruit of this hard work comes from good guidance, so I thank my project guide Prof. Dr. V. M. S. Verenkar sir for his constant supervision as well as for providing necessary information regarding the project.

I would also like to thank Goa University for providing me an opportunity to undertake this Dissertation project.

REFERENCES

- [1] S. Bayda, M. Adeel, T. Tuccinardi, M. Cordani, and F. Rizzolio, "The history of nanoscience and nanotechnology: From chemical-physical applications to nanomedicine," *Molecules*, vol. 25, no. 1. MDPI AG, 2020. doi: 10.3390/molecules25010112.
- [2] P. Thakur, D. Chahar, S. Taneja, N. Bhalla, and A. Thakur, "A review on MnZn ferrites: Synthesis, characterization and applications," *Ceramics International*, vol. 46, no. 10. Elsevier Ltd, pp. 15740–15763, Jul. 01, 2020. doi: 10.1016/j.ceramint.2020.03.287.
- [3] P. Thakur, S. Taneja, D. Chahar, B. Ravelo, and A. Thakur, "Recent advances on synthesis, characterization and high frequency applications of Ni-Zn ferrite nanoparticles," *Journal of Magnetism and Magnetic Materials*, vol. 530. Elsevier B.V., Jul. 15, 2021. doi: 10.1016/j.jmmm.2021.167925.
- [4] S. F. Shaikh, M. Ubaidullah, R. S. Mane, and A. M. Al-Enizi, "Types, Synthesis methods and applications of ferrites," in *Spinel Ferrite Nanostructures for Energy Storage Devices*, Elsevier, 2020, pp. 51–82. doi: 10.1016/b978-0-12-819237-5.00004-3.
- [5] O. Kaman *et al.*, "Structure and magnetic state of hydrothermally prepared Mn-Zn ferrite nanoparticles," *Journal of Alloys and Compounds*, vol. 888, Dec. 2021, doi: 10.1016/j.jallcom.2021.161471.
- [6] Z. Xu *et al.*, "Preparation and characterization of Mn–Zn ferrites via nano-in-situ composite method," *Solid State Sciences*, vol. 98, Dec. 2019, doi: 10.1016/j.solidstatesciences.2019.106006.
- [7] V. v. Karansky, A. S. Klimov, and S. v. Smirnov, "Structural transformations in Mn–Zn ferrite under low-energy electron beam treatment," *Vacuum*, vol. 173, Mar. 2020, doi: 10.1016/j.vacuum.2019.109115.
- [8] Z. Niu *et al.*, "Green synthesis of a novel Mn–Zn ferrite/biochar composite from waste batteries and pine sawdust for Pb²⁺ removal," *Chemosphere*, vol. 252, Aug. 2020, doi: 10.1016/j.chemosphere.2020.126529.
- [9] K. Li, C. Peng, and K. Jiang, "The recycling of Mn-Zn ferrite wastes through a hydrometallurgical route," *Journal of Hazardous Materials*, vol. 194, pp. 79–84, Oct. 2011, doi: 10.1016/j.jhazmat.2011.07.060.
- [10] C. You, X. Fan, N. Tian, and J. He, "Improved electromagnetic microwave absorption of the annealed pre-sintered precursor of Mn-Zn ferrite," *Journal of Magnetism and Magnetic Materials*, vol. 381, pp. 377–381, May 2015, doi: 10.1016/j.jmmm.2014.12.089.

- [11] P. Hu, D. Pan, S. Zhang, J. Tian, and A. A. Volinsky, "Mn-Zn soft magnetic ferrite nanoparticles synthesized from spent alkaline Zn-Mn batteries," *Journal of Alloys and Compounds*, vol. 509, no. 9, pp. 3991–3994, Mar. 2011, doi: 10.1016/j.jallcom.2010.12.204.
- [12] K. Pemartin, C. Solans, J. Alvarez-Quintana, and M. Sanchez-Dominguez, "Synthesis of Mn-Zn ferrite nanoparticles by the oil-in-water microemulsion reaction method," *Colloids and Surfaces A: Physicochemical and Engineering Aspects*, vol. 451, no. 1, pp. 161–171, Jun. 2014, doi: 10.1016/j.colsurfa.2014.03.036.
- [13] M. L. Martins, A. O. Florentino, A. A. Cavalheiro, R. I. V. Silva, D. I. dos Santos, and M. J. Saeki, "Mechanisms of phase formation along the synthesis of Mn-Zn ferrites by the polymeric precursor method," *Ceramics International*, vol. 40, no. 10, pp. 16023–16031, Dec. 2014, doi: 10.1016/j.ceramint.2014.07.137.
- [14] P. Hu *et al.*, "Heat treatment effects on microstructure and magnetic properties of Mn-Zn ferrite powders," *Journal of Magnetism and Magnetic Materials*, vol. 322, no. 1, pp. 173–177, Jan. 2010, doi: 10.1016/j.jmmm.2009.09.002.
- [15] Y. Xuan, Q. Li, and G. Yang, "Synthesis and magnetic properties of Mn-Zn ferrite nanoparticles," *Journal of Magnetism and Magnetic Materials*, vol. 312, no. 2, pp. 464–469, May 2007, doi: 10.1016/j.jmmm.2006.11.200.
- [16] M. Deepty *et al.*, "XRD, EDX, FTIR and ESR spectroscopic studies of co-precipitated Mn-substituted Zn-ferrite nanoparticles," *Ceramics International*, vol. 45, no. 6, pp. 8037–8044, Apr. 2019, doi: 10.1016/j.ceramint.2019.01.029.
- [17] M. R. Syue, F. J. Wei, C. S. Chou, and C. M. Fu, "Magnetic, dielectric, and complex impedance properties of nanocrystalline Mn-Zn ferrites prepared by novel combustion method," in *Thin Solid Films*, Sep. 2011, vol. 519, no. 23, pp. 8303–8306. doi: 10.1016/j.tsf.2011.04.003.
- [18] V. J. Angadi *et al.*, "Composition dependent structural and morphological modifications in nanocrystalline Mn-Zn ferrites induced by high energy γ -irradiation," *Materials Chemistry and Physics*, vol. 199, pp. 313–321, Sep. 2017, doi: 10.1016/j.matchemphys.2017.07.021.
- [19] M. A. Gabal, R. S. Al-luhaibi, and Y. M. al Angari, "Recycling spent zinc-carbon batteries through synthesizing nano-crystalline Mn-Zn ferrites," *Powder Technology*, vol. 258, pp. 32–37, 2014, doi: 10.1016/j.powtec.2014.03.003.
- [20] M. A. Gabal, R. S. Al-Luhaibi, and Y. M. al Angari, "Mn-Zn nano-crystalline ferrites synthesized from spent Zn-C batteries using novel gelatin method," *Journal of Hazardous Materials*, vol. 246–247, pp. 227–233, Feb. 2013, doi: 10.1016/j.jhazmat.2012.12.026.
- [21] M. A. Gabal, R. S. Al-Luhaibi, and Y. M. al Angari, "Effect of Zn-substitution on the structural and magnetic properties of Mn-Zn ferrites synthesized from spent Zn-C batteries," *Journal of Magnetism and Magnetic Materials*, vol. 348, pp. 107–112, 2013, doi: 10.1016/j.jmmm.2013.08.002.
- [22] W. Xin, C. Yinfang, W. Yongming, and L. Chunjing, "Sintering process and grain growth of Mn-Zn ferrite nanoparticles."
- [23] I. Szczygieł, K. Winiarska, A. Bieńko, K. Suracka, and D. Gaworska-Koniarek, "The effect of the sol-gel autocombustion synthesis conditions on the Mn-Zn ferrite magnetic properties,"

- Journal of Alloys and Compounds*, vol. 604, pp. 1–7, Aug. 2014, doi: 10.1016/j.jallcom.2014.03.109.
- [24] Y. Liu, J. Cao, and Z. Yang, “The structure and magnetic properties of Mn-Zn ferrite thin films fabricated by alternately sputtering,” *Materials Science and Engineering B: Solid-State Materials for Advanced Technology*, vol. 127, no. 2–3, pp. 108–111, Feb. 2006, doi: 10.1016/j.mseb.2005.09.062.
- [25] T. H. Kim *et al.*, “Reductive acid leaching of spent zinc-carbon batteries and oxidative precipitation of Mn-Zn ferrite nanoparticles,” *Hydrometallurgy*, vol. 96, no. 1–2, pp. 154–158, Mar. 2009, doi: 10.1016/j.hydromet.2008.10.001.
- [26] J. Zhang, L. Yu, S. Yuan, S. Zhang, and X. Zhao, “Abnormal morphology of nanocrystalline Mn-Zn ferrite sintered by pulse electric current sintering,” *Journal of Magnetism and Magnetic Materials*, vol. 321, no. 21, pp. 3585–3588, Nov. 2009, doi: 10.1016/j.jmmm.2009.05.045.
- [27] W. Wang, C. Zang, and Q. Jiao, “Synthesis, structure and electromagnetic properties of Mn-Zn ferrite by sol-gel combustion technique,” *Journal of Magnetism and Magnetic Materials*, vol. 349, pp. 116–120, 2014, doi: 10.1016/j.jmmm.2013.08.057.
- [28] A. C. F. M. Costa, V. J. Silva, C. C. Xin, D. A. Vieira, D. R. Cornejo, and R. H. G. A. Kiminami, “Effect of urea and glycine fuels on the combustion reaction synthesis of Mn-Zn ferrites: Evaluation of morphology and magnetic properties,” *Journal of Alloys and Compounds*, vol. 495, no. 2, pp. 503–505, Apr. 2010, doi: 10.1016/j.jallcom.2009.10.065.
- [29] M. M. Hessien, M. M. Rashad, K. El-Barawy, and I. A. Ibrahim, “Influence of manganese substitution and annealing temperature on the formation, microstructure and magnetic properties of Mn-Zn ferrites,” *Journal of Magnetism and Magnetic Materials*, vol. 320, no. 9, pp. 1615–1621, May 2008, doi: 10.1016/j.jmmm.2008.01.025.
- [30] Y. Song *et al.*, “Preparation of Zn-Mn ferrite from spent Zn-Mn batteries using a novel multi-step process of bioleaching and co-precipitation and boiling reflux,” *Hydrometallurgy*, vol. 153, pp. 66–73, 2015, doi: 10.1016/j.hydromet.2015.02.007.
- [31] A. Angermann, E. Hartmann, and J. Töpfer, “Mixed-metal carbonates as precursors for the synthesis of nanocrystalline MnZn ferrites,” *Journal of Magnetism and Magnetic Materials*, vol. 322, no. 21, pp. 3455–3459, Nov. 2010, doi: 10.1016/j.jmmm.2010.06.044.
- [32] S. Sakurai, S. Sasaki, M. Okube, H. Ohara, and T. Toyoda, “Cation distribution and valence state in Mn- Zn ferrite examined by synchrotron X-rays,” *Physica B: Condensed Matter*, vol. 403, no. 19–20, pp. 3589–3595, Oct. 2008, doi: 10.1016/j.physb.2008.05.035.
- [33] L. Xiao, T. Zhou, and J. Meng, “Hydrothermal synthesis of Mn-Zn ferrites from spent alkaline Zn-Mn batteries,” *Particuology*, vol. 7, no. 6, pp. 491–495, Dec. 2009, doi: 10.1016/j.partic.2009.04.012.
- [34] A. Yusmar, L. Armitasari, and E. Suharyadi, “Effect of Zn on dielectric properties of Mn-Zn spinel ferrite synthesized by coprecipitation,” in *Materials Today: Proceedings*, 2018, vol. 5, no. 7, pp. 14955–14959. doi: 10.1016/j.matpr.2018.04.037.